Effective interaction graphs arising from resource limitations in gene networks

Effective interaction graphs arising from resource limitations in gene networks

Yili Qian and Domitilla Del Vecchio

***Abstract*—Protein production in gene networks relies on the availability of resources necessary for transcription and translation, which are found in cells in limited amounts. As various genes in a network compete for a common pool of resources, a hidden layer of interactions among genes arises. Such interactions are neglected by standard Hill-function-based models. In this work, we develop a model with the same dimension as standard Hill-function-based models to account for the sharing of limited amounts of RNA polymerase and ribosomes in gene networks. We provide effective interaction graphs to capture the hidden interactions and find that the additional interactions can dramatically change network behavior. In particular, we demonstrate that, as a result of resource limitations, a cascade of activators can behave like an effective repressor or a biphasic system, and that a repression cascade can become bistable.**

I. INTRODUCTION

Context dependence, the unintended interactions among genetic circuits and host factors, is a current challenge in the analysis and design of biomolecular networks [1]. Such unintended interactions hinder our ability to predict design outcomes, which often leads to lengthy and *ad hoc* design processes. Therefore, much research has sought to better understand and mitigate context dependence [1], [2]. In this paper, we are concerned with the context dependence problem arising from the limitations of cellular resources. In particular, we study gene transcription networks, where genes are transcribed by RNA polymerase (RNAP) into mRNA, and mRNA is translated by ribosomes into proteins. Proteins can be transcription factors (TFs) that regulate each other by binding to the promoter site of a gene, which would either activate or repress its ability to recruit RNAP for transcription. The total amount of RNAP and ribosomes is limited and all genes simultaneously compete for these resources [3]. This limitation has been largely neglected so far, due to the small scale and simplicity of circuits considered. In larger circuits, however, the competition for limited resources has been shown to introduce interactions in gene expression levels even in the absence of explicit regulatory links [4].

In this paper, we consider general gene transcription networks and develop a modeling framework to predict the effective interactions arising from limitations in RNAP and ribosome availability. Related theoretical works have recently appeared that study resource sharing problems in biomolecular networks. De Vos et al. analyze the response of network flux toward changes in total competitors (mRNAs) and common targets (ribosomes) [5]. Yeung et al. illustrate, using tools from dynamical systems, that resource sharing leads to non-minimum phase zeros in the transfer function of a linearized genetic cascade circuit [6]. Gyorgy et al. develop the notion of realizable region for steady state gene expression under resource limitations [7]. Hamadeh et al. analyze and compare different feedback architectures to mitigate resource competition [8].

Our work focuses on the idea of effective interactions to help illustrate how sharing of RNAP and ribosomes alters the dynamics of a general gene transcription network. For example, when a TF activates the production of protein x_1, more RNAP is recruited to produce a larger number of mRNA m_1. Increased m_1 further increases the demand for ribosomes to produce x_1. Both effects decrease the amount of resources available to produce other protein species (for example, protein x_2) in the network. This waterbed effect creates an effective inhibition of protein x_2 and can be incorporated into an interaction graph, which is commonly used to describe transcriptional regulation interactions (activation/repression) among TFs.

Here, we propose a general model based on deterministic reaction rate equations and ODEs in a resource limiting environment. The model is able to account for resource limitations while maintaining the same dimension as the standard Hill-function-based models [2], [9]. Employing this model, we provide simple rules to identify the hidden interactions due to resource limitations, and the resulting effective interactions in the network. We apply our results to two-stage activation and repression cascades and illustrate how the hidden interactions can dramatically change system's behavior. In an activation cascade, resource sharing can completely invert the desired steady state I/O response or lead to biphasic behavior, while in a two-stage repression cascade, resource limitations can lead to bistability.

This paper is organized as follows. In Section II, we give a motivating example. In Section III, we introduce our general modeling framework. In Section IV, we illustrate the effective interaction graph of a general gene network. The activation and repression cascade examples are in Section V. We discuss the limitations of our approach and provide directions for future investigation in Section VI.

II. A MOTIVATING EXAMPLE

Cascade circuits are one of the most common network motifs in both natural and synthetic gene networks due to their ability to amplify signals and achieve "switch-like" behavior [9]. In Fig. 1, we consider a simple two-stage activation cascade composed of gene 1 and gene 2. Protein u is the input TF that binds with promoter p_1 to activate the production of protein x_1. Protein x_1 is an activator for the output protein (x_2). The structure of this motif can be

This work was supported by AFOSR grant FA9550-12-1-0129 and NIGMS grant P50 GMO98792.

Y. Qian and D. Del Vecchio are with the Department of Mechanical Engineering, MIT, Cambridge, MA 02139, USA. Emails: yiliqian@mit.edu (Y. Qian) and ddv@mit.edu (D. Del Vecchio).

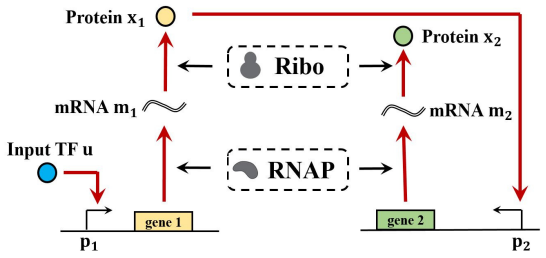

Fig. 1. A simplified diagram of a two-stage activation cascade. A limited amount of RNAP and ribosomes is shared between the two stages for the transcription of mRNAs (m_1 and m_2), and translation of proteins (x_1 and x_2), respectively.

represented by the interaction graph as $u \to x_1 \to x_2$. The dynamics of binding reactions and mRNA dynamics are often neglected because they are much faster than protein dynamics [2], [9]. We use u, x_1 and x_2 to represent the concentration of u, x_1 and x_2, respectively. In a standard model, we use Hill functions to describe gene activation, thus we have:

$$\begin{aligned} \dot{x}_1 &= \frac{\alpha_0 + \alpha(\frac{u}{k_1})^n}{1+(\frac{u}{k_1})^n} - \gamma_1 x_1, \\ \dot{x}_2 &= \frac{\beta_0 + \beta(\frac{x_1}{k_2})^m}{1+(\frac{x_1}{k_2})^m} - \gamma_2 x_2, \end{aligned} \tag{1}$$

where α_0 and β_0 are the basal production rate constants; α and β are the production rate constants with activation; k_1 and k_2 are the dissociation constants of activators u and x_1 binding with their respective promoters, γ_1 and γ_2 are the dilution/degradation rate of the proteins, and n and m are the cooperativity coefficients. Solving for the steady state of (1) gives a monotonically increasing I/O response (Fig. 2A).

To examine whether the standard model in (1) is a good representation of system response under resource limitations, we simulate the system with a mechanistic model that explicitly accounts for the usage of RNAP and ribosomes, and for their conservation law (listed in Section III). Surprisingly, simulation of this mechanistic model reveals that the steady state I/O response can be biphasic (Fig. 2B). With reference to Fig. 2A, decrease of steady state expression of x_2 with u at high input level in Fig. 2B can be explained by the following resource sharing mechanism. When promoter p_1 and mRNA m_1 have much stronger ability to sequester resources than promoter p_2 and mRNA m_2, as we increase u, the production of protein x_1 sequesters resources from the production of protein x_2, decreasing the amount of free resources available to produce x_2. When this effective repression is stronger than the activation $x_1 \to x_2$, x_2 decreases with u.

This paper is aimed to obtain an explicit model, with the same dimension as the standard model in (1), that predicts such effective interactions due to resource limitations.

III. GENERAL MODELING FRAMEWORK

A. Gene Expression in a Transcriptional Component

We consider a transcriptional component as a *node* in the gene network [10]. A transcriptional component takes a number of TFs to bind with its gene promoter p_i and triggers a series of chemical reactions to produce a TF x_i as output. The input TFs can either activate or repress the expression of gene i by changing the binding strength of p_i with RNAP.

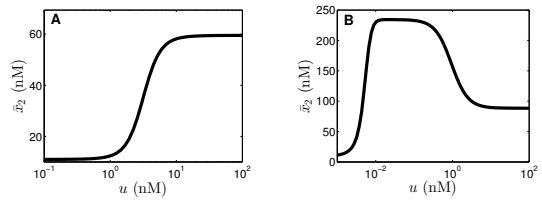

Fig. 2. $\bar{x}_2$ is the steady state concentration of protein x_2. (A) According to the standard model, steady state output $\bar{x}_2$ increases with input u. (B) However, simulation using ODEs (2) to (8) and conservation of resources shows that system response can be biphasic. Simulation parameters in the standard model in equation (1): $\alpha_0 = \beta_0 = 1\,(\mathrm{hr})^{-1}$; $\alpha = \beta = 100\,(\mathrm{hr})^{-1}$; $k_1 = k_2 = 10\,(\mathrm{nM})^2$, $\gamma_1 = \gamma_2 = 1\,(\mathrm{hr})^{-1}$ and $n = m = 2$. Simulation parameters in the full mechanistic model are in Table II.

Since most gene promoters take at most two input TFs [2] [9], we consider a node i taking two input TFs (x_1 and x_2) that form complexes with p_i. The reactions are:

$$\mathrm{p_i} + n_1 \cdot \mathrm{x_1} \underset{\mathrm{k_1^-}}{\overset{\mathrm{k_1^+}}{\rightleftharpoons}} \mathrm{c_i^1}, \qquad \mathrm{p_i} + n_2 \cdot \mathrm{x_2} \underset{\mathrm{k_2^-}}{\overset{\mathrm{k_2^+}}{\rightleftharpoons}} \mathrm{c_i^2},$$

$$\mathrm{c_i^1} + n_2 \cdot \mathrm{x_2} \underset{\mathrm{k_{12}^-}}{\overset{\mathrm{k_{12}^+}}{\rightleftharpoons}} \mathrm{c_i^{12}}, \qquad \mathrm{c_i^2} + n_1 \cdot \mathrm{x_1} \underset{\mathrm{k_{21}^-}}{\overset{\mathrm{k_{21}^+}}{\rightleftharpoons}} \mathrm{c_i^{12}},$$

where n_1 and n_2 are the cooperativities of x_1 and x_2 binding with p_i, respectively. The promoter p_i and the promoter/TF complexes (c_i^1, c_i^2, c_i^{12}) recruit free RNAP (y) to form an open complex for transcription. The reactions are given by:

$$\mathrm{p_i} + \mathrm{y} \underset{\mathrm{d'}}{\overset{\mathrm{a'}}{\rightleftharpoons}} \mathrm{C_i}, \qquad \mathrm{c_i^j} + \mathrm{y} \underset{\mathrm{d_j}}{\overset{\mathrm{a_j}}{\rightleftharpoons}} \mathrm{C_i^j}\ (\mathrm{j} = 1, 2, 12).$$

These transcriptionally active complexes can then be transcribed into mRNA (m_i), with reactions given by:

$$\mathrm{C_i} \xrightarrow{\alpha_0} \mathrm{p_i} + \mathrm{y} + \mathrm{m_i}, \quad \mathrm{C_i^j} \xrightarrow{\alpha_j} \mathrm{c_i^j} + \mathrm{y} + \mathrm{m_i}\ (\mathrm{j} = 1, 2, 12).$$

Translation is initiated by ribosomes (z) binding with the ribosome binding site (RBS) on mRNA m_i to form a translationally active complex M_i, which is then translated into protein x_i. Meanwhile, mRNA and proteins are also diluted/degraded. The reactions are:

$$\mathrm{m_i} + \mathrm{z} \underset{\kappa^-}{\overset{\kappa^+}{\rightleftharpoons}} \mathrm{M_i}, \qquad \mathrm{M_i} \xrightarrow{\theta_i} \mathrm{m_i} + \mathrm{z} + \mathrm{x_i},$$

$$\mathrm{m_i} \xrightarrow{\delta_i} \emptyset, \qquad \mathrm{M_i} \xrightarrow{\omega_i} \mathrm{z}, \qquad \mathrm{x_i} \xrightarrow{\gamma_i} \emptyset.$$

Consequently, we have the following ODEs in node i:

$$\dot{c}_i^j = k_j^+ p_i x_j^{n_j} - k_j^- c_i^j - a_j y c_i^j + d_j C_i^j + \alpha_j C_i^j, \tag{2}$$

$$\begin{aligned} \dot{c}_i^{12} &= k_{12}^+ c_i^1 x_2^{n_2} - k_{12}^- c_i^{12} + k_{21}^+ c_i^2 x_1^{n_1} - k_{21}^- c_i^{12} \\ &\quad - a_{12} c_i^{12} y - d_{12} C_i^{12} + \alpha_{12} C_i^{12}, \end{aligned} \tag{3}$$

$$\dot{C}_i = a^{'} p_i y - d^{'} C_i - \alpha_0 C_i, \tag{4}$$

$$\dot{C}_i^k = a_k y c_i^k - d_k C_i^k - \alpha_k C_i^k, \tag{5}$$

$$\begin{aligned} \dot{m}_i &= \alpha_0 C_i + \alpha_1 C_i^1 + \alpha_2 C_i^2 + \alpha_{12} C_i^{12} \\ &\quad - \delta_i m_i - \kappa^+ m_i z + \kappa^- M_i + \theta_i M_i, \end{aligned} \tag{6}$$

$$\dot{M}_i = \kappa^+ m_i z - \kappa^- M_i - \theta_i M_i - \omega_i M_i, \tag{7}$$

$$\dot{x}_i = \theta_i M_i - \gamma_i x_i, \tag{8}$$

where indices $j = 1, 2$ and $k = 1, 2, 12$. Since DNA concentration is conserved [9], we have

$$p_{i,T} = p_i + C_i + \sum_{j=1,2,12} (c_i^j + C_i^j), \tag{9}$$

where $p_{i,T}$ is the total concentration of gene i. Given that the binding reactions and mRNA dynamics are much faster than protein production and degradation [9], we can set (2) to (7) to quasi-steady state (QSS) to simplify our analysis.

We first obtain the QSS concentration of complexes formed with $\mathrm{p_i}$:

$$c_i^1 = \frac{p_i x_1^{n_1}}{k_i^1}, c_i^2 = \frac{p_i x_2^{n_2}}{k_i^2}, c_i^{12} = \frac{p_i x_1^{n_1} x_2^{n_2}}{k_i^1 k_i^{12}} + \frac{p_i x_1^{n_1} x_2^{n_2}}{k_i^2 k_i^{21}},$$

$$C_i = \frac{p_i y}{K_i'}, \qquad C_i^j = \frac{c_i^j y}{K_i^j} \ (j = 1, 2, 12), \tag{10}$$

where dissociation constants are defined as:

$$K_i' = \frac{d' + \alpha_0}{a'}, \quad K_i^j = \frac{d_j + \alpha_j}{a_j}, \quad k_i^j = \frac{k_j^-}{k_j^+} \ (j = 1, 2, 12).$$

Here, K_i' is the basal dissociation constant of promoter $\mathrm{p_i}$ with RNAP y, K_i^j is the dissociation constant of promoter/TF complex $\mathrm{c_i^j}$ with y, and k_i^j is the dissociation constant of TF $\mathrm{x_j}$ binding with $\mathrm{p_i}$. A smaller dissociation constant indicates stronger binding. When node i takes only one input, for simplicity, we write K_i for K_i^1 and k_i for k_i^1. To obtain the QSS concentration of mRNA complexes, we further assume that the transcription rates are independent of how transcriptions are initiated and thus $\alpha_0 = \alpha_1 = \alpha_2 = \alpha_{12}$. We can then substitute (10) into the QSS of ODEs (6) and (7) and obtain

$$M_i = \frac{\alpha_i}{\delta_i} \frac{z}{\kappa_i} (C_i + \sum_j C_i^j) = \frac{\alpha_i p_{i,T}}{\delta_i} \frac{z}{\kappa_i} \frac{y}{K_i'} F_i(\mathbf{u}_i), \tag{11}$$

where vector $\mathbf{u}_i = [x_1, x_2]^T$ and index $j = 1, 2, 12$. $\kappa_i = (\kappa^- + \theta_i + \omega_i)/\kappa^+$ is the dissociation constant of $\mathrm{m_i}$ binding with ribosomes z. A smaller κ_i indicates stronger RBS strength. $F_i(\mathbf{u}_i) : \mathbb{R}^2 \mapsto \mathbb{R}$ is the Hill function derived by substituting (10) into the DNA conservation law in (9) and solving for $C_i + C_i^1 + C_i^2 + C_i^{12}$. Assuming that the free amount of RNAP and ribosomes are limited, in particular,

$$y \ll K_i, K_i' \qquad \text{and} \qquad z \ll \kappa_i, \tag{12}$$

$F_i(\mathbf{u}_i)$ can be written as:

$$F_i(\mathbf{u}_i) = \frac{1 + a_i^1 x_1^{n_1} + a_i^2 x_2^{n_2} + a_i^3 x_1^{n_1} x_2^{n_2}}{1 + b_i^1 x_1^{n_1} + b_i^2 x_2^{n_2} + b_i^3 x_1^{n_1} x_2^{n_2}}, \tag{13}$$

where

$$a_i^1 = \frac{K_i'}{K_i^1 k_i^1}, \ a_i^2 = \frac{K_i'}{K_i^2 k_i^2}, \ a_i^3 = \frac{K_i'}{K_i^{12}} \left(\frac{1}{k_i^1 k_i^{12}} + \frac{1}{k_i^2 k_i^{21}} \right),$$

$$b_i^1 = \frac{1}{k_i^1}, \ b_i^2 = \frac{1}{k_i^2}, \ b_i^3 = \frac{1}{k_i^1 k_i^{12}} + \frac{1}{k_i^2 k_i^{21}}. \tag{14}$$

Situations in (12), where resources are limited, are described in the Appendix. Finally, we combine equation (11) and (8) to obtain the dynamics of x_i:

$$\dot{x}_i = \frac{\alpha_i \theta_i p_{i,T}}{\delta_i} \cdot \frac{y}{K_i'} \cdot \frac{z}{\kappa_i} \cdot F_i(\mathbf{u_i}) - \gamma_i \cdot x_i. \tag{15}$$

Since y and z are shared among all nodes in the network, their free concentrations y, z need to be determined from the network context. This is the aim of the next subsection.

B. Resource Sharing in Gene Networks

A gene network $\mathcal{N}$ is composed of N nodes and L external TF inputs $(\mathrm{v_1}, \cdots, \mathrm{v_L})$. The concentration of the external inputs can be represented by $\mathbf{v} = [v_1, \cdots, v_L]^T$ and the state of the network is represented by the concentrations of output proteins of each node $\mathbf{x} = [x_1, \cdots, x_N]^T$. The set of all TFs in the network is $\mathcal{X} = \{\mathrm{x_1}, \cdots, \mathrm{x_N}, \mathrm{v_1}, \cdots, \mathrm{v_L}\}$, and we use $\boldsymbol{\xi} = [\mathbf{x}^T, \mathbf{v}^T]^T$ to represent the vector of their concentrations. Nodes can be connected by transcriptional regulation interactions where protein $\mathrm{x_j}$ can either activate or repress the production of $\mathrm{x_i}$ by binding to its promoter. We call $\mathrm{x_i}$ as a *target* of $\mathrm{x_j}$ and $\mathrm{x_j}$ as a *parent* of $\mathrm{x_i}$. We denote by $\mathcal{U}_i \subseteq \mathcal{X}$ the set of all parents of $\mathrm{x_i}$. Their concentrations are given by a vector $\mathbf{u}_i = Q_i \cdot \boldsymbol{\xi}$, where elements in Q_i are defined as:

$$q_{jk} = \begin{cases} 1, & \text{if } \xi_k \text{ is the } j\text{th input to node i,} \\ 0, & \text{otherwise.} \end{cases} \tag{16}$$

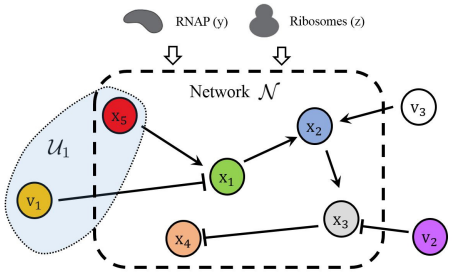

Fig. 3. In this example network, $\mathbf{x} = [x_1, \cdots, x_5]^T$ and $\mathbf{v} = [v_1, v_2, v_3]^T$. $\mathcal{X} = \{\mathrm{x_1}, \cdots \mathrm{x_5}, \mathrm{v_1}, \mathrm{v_2}, \mathrm{v_3}\}$. Using node 1 as an example, we have $\mathcal{U}_1 = \{\mathrm{x_5}, \mathrm{v_1}\}$, $\mathbf{u_1} = [x_5, v_1]^T$. A constant amount of RNAP and ribosomes are available for nodes 1 to 5. Links between nodes indicate transcriptional regulation interactions, where "$\rightarrow$" is an activation and "$\dashv$" is a repression.

Fig. 3 illustrates an example gene network. To determine the effect of RNAP and ribosome limitations on the gene network, we account for the fact that the total amount of resources available to network $\mathcal{N}$ is constant [3]:

$$y_T = y + \sum_{i=1}^{N} y_i, \qquad z_T = z + \sum_{i=1}^{N} z_i, \tag{17}$$

where y_T and z_T represent the total amount of RNAP and ribosomes, respectively. We let $\mathrm{y_i}$ and $\mathrm{z_i}$ denote the RNAP and ribosomes bound to (used by) node i, thus $y_i = C_i + C_i^1 + C_i^2 + C_i^{12}$, and $z_i = M_i$. According to (11), we have:

$$y_i = p_{i,T} \frac{y}{K_i'} F_i(\mathbf{u}_i), \quad z_i = \frac{\alpha_i p_{i,T}}{\delta_i} \frac{y}{K_i'} \frac{z}{\kappa_i} F_i(\mathbf{u}_i). \tag{18}$$

Combining equation (17) and (18), we obtain:

$$y = \frac{y_T}{1 + \sum_{i=1}^{N} [\frac{p_{i,T}}{K_i'} F_i(\mathbf{u}_i)]}, \quad z = \frac{z_T}{1 + y \sum_{i=1}^{N} [\frac{\alpha_i p_{i,T}}{\delta_i K_i' \kappa_i} F_i(\mathbf{u}_i)]}.$$

Hence,

$$y \cdot z = \frac{y_T \cdot z_T}{1 + \sum_{i=1}^{N} \frac{p_{i,T}}{K_i'} \cdot (1 + \frac{\alpha_i}{\kappa_i \delta_i} y_T) \cdot F_i(\mathbf{u}_i)}. \tag{19}$$

Substituting (19) into (15), the dynamics of x_i are given by:

$$\dot{x}_i = \frac{T_i F_i(\mathbf{u}_i)}{1 + \sum_{k=1}^{N} J_k F_k(\mathbf{u}_k)} - \gamma_i x_i, \tag{20}$$

where J_i and T_i are lumped parameters defined as:

$$J_i := \frac{p_{i,T}}{K_i'} \cdot (1 + \frac{\alpha_i}{\kappa_i \delta_i} y_T), T_i := y_T z_T p_{i,T} \cdot \frac{\theta_i \alpha_i}{K_i' \kappa_i \delta_i}. \tag{21}$$

$F_i(\mathbf{u}_i)$ is the only element in equation (20) that reflects transcriptional regulations on node i. According to equation (13), the form of $F_i(\mathbf{u}_i)$ is the same as those of the standard Hill functions described in [2] and [9]. Note that $F_i(\mathbf{u}_i) \equiv 1$ when $\mathbf{u}_i = \mathbf{0}$, hence, according to (15), T_i represents the "baseline" gene expression of node i, because T_i is the production rate of $\mathrm{x_i}$ when $\mathbf{u}_i = \mathbf{0}$, $y = y_T$ and $z = z_T$.

C. J_i as a Measure of Resource Usage by Node i

J_i is a constant for node i that defines its "baseline" resource usage when $\mathbf{u}_i = \mathbf{0}$. We take J_i as a measure of resource usage by node i because the expression in (19) implies the "conservation law" for $y \cdot z$:

$$y_T \cdot z_T = \underbrace{y \cdot z}_{\text{free resources}} + \sum_{i=1}^{N} \underbrace{(J_i \cdot F_i(\mathbf{u}_i) \cdot y \cdot z)}_{\text{resource used by node } x_i}. \quad (22)$$

Furthermore, the only difference between our modified model in equation (20) and the standard no-resource-sharing model in [2] and [9] is the denominator term $D = 1 + \sum_{k=1}^{N} J_k F_k(\mathbf{u}_k)$. The following claim shows that when resources used by every node in $\mathcal{N}$ are negligible, the resource usage measure $J_i \ll 1$.

Claim 1: For every $\mathbf{u}_i$, if $y_i \ll y$ and $z_i \ll z$ for all $i = 1, \cdots, N$, then $J_i \ll 1$ for all $i = 1, \cdots, N$.

Proof: Using equation (18), $y_i \ll y$ for every $\mathbf{u}_i$ is equivalent to $p_{i,T} F_i(\mathbf{u}_i)/K_i^{'} \ll 1$ for every $\mathbf{u}_i$. Thus, we must have $p_{i,T}/K_i^{'} \ll 1$. Similarly, $z_i \ll z$ for every $\mathbf{u}_i$ requires $\frac{\alpha_i p_{i,T} y}{\delta_i K_i' \kappa_i} \ll 1$. Since $y_i \ll y$ for all i, $y \approx y_T$. Therefore, $\frac{\alpha_i p_{i,T} y_T}{\delta_i K_i' \kappa_i} \ll 1$ and $J_i \ll 1$ for all i. ■

This claim shows that when resource usage is negligible in the network, $0 < J_i \ll 1$ $(i = 1, \cdots, N)$ and the modified model reduces back to the standard model in [2] and [9]:

$$\dot{x}_i = T_i F_i(\mathbf{u}_i) - \gamma_i x_i. \quad (23)$$

Equation (21) indicates that a node i is a strong resource sink when $\mathbf{u}_i = \mathbf{0}$ (J_i is large) if its (i) copy number is large; (ii) basal RNAP sequestering capability is strong (small K_i'); (iii) transcription rate constant is large; (iv) ribosome sequestering capability is strong (small κ_i); (v) mRNA degradation rate is low and (vi) the total amount of RNAP is large. Conditions (i) and (ii) are associated with the $p_{i,T}/K_i'$ term in equation (21), and describe the node's capability to sequester RNAP. Conditions (iii) to (vi) are the contributions from the $(\alpha_i y_T)/(\kappa_i \delta_i)$ term and characterize the node's capability to sequester free ribosomes.

IV. EFFECTIVE INTERACTIONS DUE TO RESOURCE LIMITATIONS

Directed edges, such as those in Fig. 3, have been used to represent transcriptional regulation interactions, where one TF binds with the promoters of its targets to regulate the target's production [9]. Here, we mathematically define the standard to draw interaction graphs and illustrate that resource limitations lead to effective interactions in gene networks that do not rely on TF regulation.

Definition 1: Let the dynamics of x_i be given by $\dot{x}_i = G_i(\boldsymbol{\xi}) - \gamma_i \cdot x_i$. We draw the interaction graph from TF ξ_{j} to $\mathrm{x_i}$ based on the following rules:

- If $\frac{\partial G_i}{\partial \xi_j} \equiv 0$ for all $\xi_j \in \mathbb{R}^+$, then there is no interaction from ξ_{j} to $\mathrm{x_i}$;
- If $\frac{\partial G_i}{\partial \xi_j} \geq 0$ for all $\xi_j \in \mathbb{R}^+$ and $\frac{\partial G_i}{\partial \xi_j} \neq 0$ for some ξ_j, then ξ_{j} activates $\mathrm{x_i}$ and we draw $\xi_{\mathrm{j}} \rightarrow \mathrm{x_i}$;
- If $\frac{\partial G_i}{\partial \xi_j} \leq 0$ for all $\xi_j \in \mathbb{R}^+$ and $\frac{\partial G_i}{\partial \xi_j} \neq 0$ for some ξ_j, then ξ_{j} represses $\mathrm{x_i}$ and we draw $\xi_{\mathrm{j}} \dashv \mathrm{x_i}$.
- If $\frac{\partial G_i}{\partial \xi_j} \geqslant 0$ for some $\xi_j \in \mathbb{R}^+$ and $\frac{\partial G_i}{\partial \xi_j} < 0$ for some other ξ_j, then the regulation of ξ_{j} on $\mathrm{x_i}$ is undetermined and we draw $\xi_{\mathrm{j}} \multimap \mathrm{x_i}$;

Based on Definition 1, for the standard model in equation (23), $G_i(\boldsymbol{\xi}) = T_i F_i(Q_i \boldsymbol{\xi}) = T_i F_i(\mathbf{u}_i)$, and therefore there is a link from ξ_{j} to $\mathrm{x_i}$ if and only if $\xi_{\mathrm{j}} \in \mathcal{U}_i$. In our modified model in equation (20), instead we have

$$G_i(\boldsymbol{\xi}) = \frac{T_i F_i(Q_i \cdot \boldsymbol{\xi})}{1 + \sum_{k=1}^{N} J_k F_k(Q_k \cdot \boldsymbol{\xi})} = \frac{T_i F_i(\mathbf{u}_i)}{1 + \sum_{k=1}^{N} J_k F_k(\mathbf{u}_k)},$$

which implies that the dynamics of x_i may be influenced by TFs that do not belong to its parents $\mathcal{U}_i$.

In what follows, we discuss the effective interactions from $\xi_{\mathrm{j}} \in \chi$ to protein $\mathrm{x_i}$ when (i) $\mathrm{x_i}$ is the only target of ξ_{j}, (ii) $\mathrm{x_i}$ is one of the multiple targets of ξ_{j}, and (iii) $\mathrm{x_i}$ is not a target of ξ_{j}. We do not require $\mathrm{x_i} \neq \xi_{\mathrm{j}}$ and assume that a TF cannot be both an activator and a repressor. When $\mathrm{x_i}$ is the only target of ξ_{j}, the following claim shows that resource limitations do not alter the activation/repression of $\mathrm{x_i}$ by ξ_{j} in the interaction graph.

Claim 2: If $\xi_{\mathrm{j}} \in \mathcal{U}_i$ and $\xi_{\mathrm{j}} \notin \mathcal{U}_q$ for all $(q \neq i)$. Then we have $\mathrm{sign}[\partial G_i(\boldsymbol{\xi})/\partial \xi_j] = \mathrm{sign}[\partial F_i(Q_i \boldsymbol{\xi}))/\partial \xi_j]$.

Proof: According to equation (20),

$$\frac{\partial G_i(\boldsymbol{\xi})}{\partial \xi_j} = \overbrace{\frac{\partial G_i}{\partial F_i}}^{\text{positive}} \cdot \frac{\partial F_i(Q_i \boldsymbol{\xi})}{\partial \xi_j} \Rightarrow \mathrm{sign}\left(\frac{\partial G_i}{\partial \xi_j}\right) = \mathrm{sign}\left(\frac{\partial F_i}{\partial \xi_j}\right).$$

■

Remark 1: In the case where $\xi_{\mathrm{j}} \in \mathcal{U}_1, \cdots, \mathcal{U}_k$ $(k \geq 2)$, the effective interactions from ξ_{j} to its targets are undetermined. For example, if ξ_{j} represses $\mathrm{x_1}$ and $\mathrm{x_2}$ simultaneously, the effective interaction from ξ_{j} to $\mathrm{x_1}$ is given by

$$\frac{\partial G_1(\boldsymbol{\xi})}{\partial \xi_j} = \underbrace{\frac{\partial G_1}{\partial F_1}}_{\text{positive}} \cdot \overbrace{\underbrace{\frac{\partial F_1(Q_1 \boldsymbol{\xi})}{\partial \xi_j}}_{\text{negative}}}^{\text{transcriptional repression}} + \overbrace{\underbrace{\frac{\partial G_1}{\partial F_2}}_{\text{negative}} \cdot \underbrace{\frac{\partial F_2(Q_2 \boldsymbol{\xi})}{\partial \xi_j}}_{\text{negative}}}^{\text{hidden activation}}.$$

As $\mathrm{sign}(\partial G_1/\partial \xi_j)$ cannot be determined, the effective interaction from ξ_{j} to $\mathrm{x_1}$ is undetermined.

When ξ_{j} is not a parent of $\mathrm{x_i}$, the following claim shows ξ_{j} is an effective repressor for $\mathrm{x_i}$ if ξ_{j} is an activator. Conversely, ξ_{j} is an effective activator for $\mathrm{x_i}$ if it is a repressor.

Claim 3: If $\xi_j \notin \mathcal{U}_i$ but $\xi_j \in \mathcal{U}_k$ for some $k \neq i$, then we have $\mathrm{sign}[\partial G_i(\boldsymbol{\xi})/\partial \xi_j] = -\mathrm{sign}[\partial F_k(Q_k \boldsymbol{\xi})/\partial \xi_j]$.

Proof: Since $\xi_j \notin \mathcal{U}_i$, $\partial G_i/\partial F_k < 0$ for all k.

$$\frac{\partial G_i(\boldsymbol{\xi})}{\partial \xi_j} = \sum_k \underbrace{\frac{\partial G_i}{\partial F_k}}_{\text{negative}} \cdot \frac{\partial F_k(Q_k \boldsymbol{\xi})}{\partial \xi_j}.$$

Therefore, $\mathrm{sign}(\partial G_i/\partial \xi_j) = -\mathrm{sign}(\partial F_k/\partial \xi_j)$. ■

The effective interactions for the above three cases are summarized in Table I, with illustrative examples given in each case. For any index $i, j \in \{1, \cdots, N\}$, a black solid line from node j to node i represents $\partial F_i(Q_i \boldsymbol{\xi})/\partial \xi_j$, the interaction due to transcriptional regulation, while a red dashed line represents any hidden (additional) interactions arising from $\partial G_i(\boldsymbol{\xi})/\partial \xi_j$.

TABLE I. EFFECTIVE INTERACTIONS WITH RESOURCE LIMITATIONS

Remark 1	***Claim*** 2	***Claim*** 3
ξ_j to multiple targets	ξ_j to its only target	ξ_j to nodes that are NOT its target
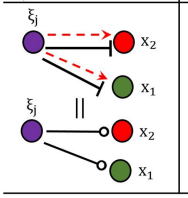	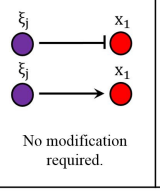 No modification required.	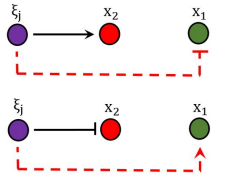

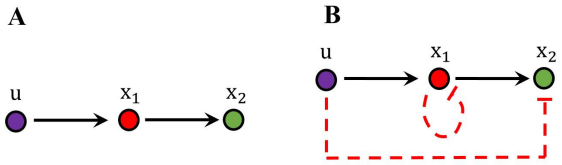

Fig. 4. In addition to the regulatory transcriptional activations (solid lines) captured by the ideal model in equation (1) (A), resource limitations introduce two hidden repressions (dashed lines) into the system: repression from input u to output x_2 and negative auto-regulation of x_1 (B).

V. APPLICATION TO ACTIVATION AND REPRESSION CASCADES

A. Two-stage Activation Cascade

We first revisit the motivating example in Section II. u is the input and x_1 and x_2 are the two TFs cascaded by transcriptional regulation interactions (Fig. 4A). According to (20), the dynamics of the system can be written as:

$$\begin{aligned}\dot{x}_1 &= \underbrace{\frac{T_1F_1(u)}{1+J_1F_1(u)+J_2F_2(x_1)}}_{G_1(u,x_1)} - \gamma_1 x_1,\\ \dot{x}_2 &= \underbrace{\frac{T_2F_2(x_1)}{1+J_1F_1(u)+J_2F_2(x_1)}}_{G_2(u,x_1)} - \gamma_2 x_2.\end{aligned} \tag{24}$$

From (13) and (14) we have:

$$F_1(u) = \frac{1+a_1^1u^n}{1+b_1^1u^n}, \qquad F_2(x_1) = \frac{1+a_2^1x_1^m}{1+b_2^1x_1^m}.$$

From Claim 3, since u is an activator, there is a hidden repression from u to x_2. Similarly, there is a hidden negative auto-regulation on x_1. These hidden interactions are represented by dashed lines in Fig. 4B. From Claim 2, since u and x_1 both have only one target, we draw u $\rightarrow$ x_1 and $x_1 \rightarrow x_2$ in Fig. 4B. The effective interaction graph of the activation cascade becomes that of an incoherent feed-forward loop (IFFL) [9]. The steady state I/O response of an IFFL can, depending on parameters, be qualitatively characterized by monotonically increasing, monotonically decreasing or biphasic functions [9] [11]. We show the simulation of steady state response of activation cascades in Fig. 5. Decreasing steady state response occurs when (a) resources are limited (large DNA copy number) and (b) x_1 has stronger resource sequestering capability than x_2 (stronger RBS). The numerical result is in agreement with the following analytical results providing sufficient conditions for different steady state I/O responses.

Claim 4: If node 1 and 2 have the same DNA copy numbers $p_{1,T} = p_{2,T} = p_T$, and transcription rate constants $\alpha_1 = \alpha_2 = \alpha$, then in a two-stage activation cascade the slope of the steady state I/O response $d\bar{x}_2/du$ satisfies:

1) $d\bar{x}_2/du > 0$ for all $u > 0$ if (a) $K_1 \gg p_T$ and (b) $\kappa_1 \cdot \delta_1 \gg \alpha \cdot y_T$;
2) $d\bar{x}_2/du < 0$ for all $u > 0$ if (a) $p_T \gg K_2^{'} > K_2 \gg K_1^{'} > K_1$ and (b) $\alpha \cdot y_T \gg \delta_2 \cdot \kappa_2 \gg \delta_1 \cdot \kappa_1$;
3) $d\bar{x}_2/du > 0$ when $u \rightarrow 0$ and $d\bar{x}_2/du < 0$ when $u \rightarrow \infty$ if (a) $K_1^{'} \gg p_T \geq K_2 \gg K_1$ and (b) $\kappa_2 \cdot \delta_2 > \kappa_1 \cdot \delta_1 \gg \alpha \cdot y_T$.

The proof consists of solving the steady state concentration of the output $\bar{x}_1$ and $\bar{x}_2$ from (24), and then apply the parameter conditions to simplify their expressions.

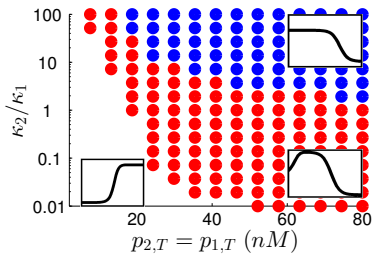

Fig. 5. Numerical simulation of $d\bar{x}_2/du$ for different DNA copy numbers and relative ribosome binding strengths (κ_2/κ_1). The uncolored region indicates $d\bar{x}_2/du > 0$ for all simulated u (monotonically increasing response). The region with red dots represent parameters where $d\bar{x}_2/du$ becomes negative at high input levels (biphasic response), and the region with blue dots represent parameters that give $d\bar{x}_2/du < 0$ for all input levels (monotonically decreasing response). Simulation parameters are shown in Table II

B. Two-stage Repression Cascade

A two-stage repression cascade consists of two repressors: TF u is the repressor for protein x_1, and x_1 is a repressor for output protein x_2 (Fig. 6A). A repressor inhibits the production of its target by binding with its promoter region, thus inhibiting RNAP (y) recruitment. A repression cascade is expected to have a unique steady state and a monotonically increasing I/O response [9]. Here, we apply our modified model to investigate its behavior under resource limitations. In our model, the inputs to the two nodes are $\mathcal{U}_1 =$ u and $\mathcal{U}_2 = x_1$, respectively. Using the results in (20), the two-stage repression cascade can be modeled as:

$$\begin{aligned}\dot{x}_1 &= \underbrace{\frac{T_1F_1(u)}{1+J_1F_1(u)+J_2F_2(x_1)}}_{G_1(u,x_1)} - \gamma_1 x_1,\\ \dot{x}_2 &= \underbrace{\frac{T_2F_2(x_1)}{1+J_1F_1(u)+J_2F_2(x_1)}}_{G_2(u,x_1)} - \gamma_2 x_2.\end{aligned} \tag{25}$$

For simplicity, we assume that the repressors are not leaky such that when u or x_1 are bound to the promoters of their targets, y can not bind with the promoters. From (14) and (13), we have:

$$F_1(u) = \frac{1}{1+\frac{1}{k_1}u^n}, \qquad F_2(x_1) = \frac{1}{1+\frac{1}{k_2}x_1^m}.$$

From Claim 3, we find that there is a hidden activation of x_2 by u and a hidden positive auto-regulation on x_1. Positive feedback loops like the one in Fig. 6B have been

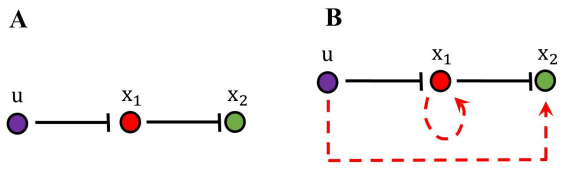

Fig. 6. In addition to transcriptional repressions (solid lines) in (A), resource limitations introduce two hidden activations (dashed lines) into the system (B): activation from u to x_2 and positive auto-regulation of x_1.

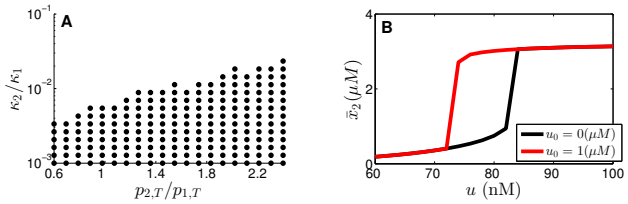

Fig. 7. (A): Dots indicate paramters that admit three solutions to equation (28), and thus lead to bistability in some input ranges. Bistability occurs when node 2 has strong capability to sequester resources (high copy number and ribosome binding strength). (B): When simulation starts from no induction ($u_0 = 0$) and full induction ($u_0 = 1(\mu\text{M})$), system steady state response show hysteresis. Simulation parameters for both cases are shown in Table II.

closely related to bistable behaviors theoretically [12], and bimodal reporter gene distributions experimentally [13]. In order to determine whether the repression cascade can display bistability because of this positive auto-regulation, we perform nullcline analysis. The two nullcline equations of the nonlinear system (25) at equilibrium $\bar{\mathbf{x}} = [\bar{x}_1, \bar{x}_2]^T$ and constant input $\bar{u}$ (and thus, constant $F_1(\bar{u})$) are given by:

$$\frac{T_1 F_1(\bar{u})}{1 + J_1 F_1(\bar{u}) + J_2 F_2(\bar{x}_1)} - \gamma_1 \bar{x}_1 = 0, \tag{26}$$

$$\frac{T_2 F_2(\bar{x}_1)}{1 + J_1 F_1(\bar{u}) + J_2 F_2(\bar{x}_1)} - \gamma_2 \bar{x}_2 = 0. \tag{27}$$

Equation (26) is a single variable equation of $\bar{x}_1$, and equation (27) defines a unique $\bar{x}_2$ for every $\bar{x}_1$. Therefore, the number of equilibria of this nonlinear system is solely determined by equation (26) which can be re-written as:

$$h_1(\bar{x}_1) = \frac{T_1 F_1(\bar{u})}{1 + J_1 F_1(\bar{u}) + J_2 F_2(\bar{x}_1)} = h_2(\bar{x}_1) = \gamma_1 \bar{x}_1. \tag{28}$$

Since $h_1(\bar{x}_1)$ is an increasing Hill function and $h_2(\bar{x}_1)$ is an increasing linear function, they can have either 1 or 3 intersections when the cooperativity $m > 1$. Particularly, when there exists $\bar{x}_1^1 < \bar{x}_1^2 < \bar{x}_1^3$ satisfying $h_1(\bar{x}_1^k) = h_2(\bar{x}_1^k)$ $(k = 1, 2, 3)$, $\bar{x}_1^1$ and $\bar{x}_1^3$ are locally stable nodes and $\bar{x}_1^2$ is a saddle point.

Now we seek to obtain parameter conditions that give rise to a bistable repression cascade. To do this, we utilize the following claim showing that the nonlinear repression cascade is bistable if and only if its linearized system is unstable at some equilibrium.

***Claim** 5:* For a given input u^*, let $\mathbf{x}^*$ be one of the corresponding equilibria. The nonlinear system (25) is bistable if and only if $-\gamma_1 + \frac{\partial G_1}{\partial x_1}\Big|_{\mathbf{x}^*, u^*} > 0$ for some $(\mathbf{x}^*, u^*)$.

Proof: (sketch) Note that $\lambda_1 = -\gamma_1 + \frac{\partial G_1}{\partial x_1}\Big|_{\mathbf{x}^*, u^*}$ and $\lambda_2 = -\gamma_2 < 0$ are the two eigenvalues of the linearization of nonlinear system (25) at $(\mathbf{x}^*, u^*)$. The linearized system is unstable if and only if $\lambda_1 > 0$.
($\Rightarrow$) When the nonlinear system is bistable at input u^*, according to our nullcline analysis, there are 3 equilibria: 2 stable nodes and a saddle point. Linearizing the system around the saddle point yields an unstable linearized system.
($\Leftarrow$) We let $H(x_1, u) = G_1(x_1, u) - \gamma_1 x_1$, at fixed $u = u^*$, with abuse of notation, we write $H(x_1) = H(x_1, u^*)$. $H(x_1)$ is continuously differentiable and solution to $H(x_1) = 0$ entirely determines the number of equilibria. When $\lambda_1(x_1^*, u^*) = H'(x_1^*) > 0$, since $H(x_1^*) = 0$, by continuity, there exists $\epsilon > 0$ such that $H(x_1 - \epsilon) < 0$ and $H(x_1 + \epsilon) > 0$. Also, when $x_1 = 0$, $H(0) = G_1(0) > 0$, and when $x_1 \to \infty$, $H(x_1) \to -\infty$. According to the intermediate value theorem, there exist a x_1^{*-} such that $0 < x_1^{*-} < x_1 - \epsilon$ and satisfies $H(x_1^{*-}) = 0$. Similarly, there exists a x_1^{*+} such that $x_1 + \epsilon < x_1^{*+}$ and satisfies $H(x_1^{*+}) = 0$. Since there are at most three zeros to the equation $H(x_1) = 0$, $H'(x_1^{*-})$ and $H'(x_1^{*+})$ are negative, and thus they are stable. ■

Remark 2: To obtain a bistable cascade, we need

$$\lambda_1 = -\gamma_1 + \frac{\partial G_1}{\partial x_1} = -\gamma_1 - \frac{T_1 J_2 F_1(u^*) \frac{\partial F_2(x_1^*)}{\partial x_1}}{[1 + J_1 F_1(x_1^*) + J_2 F_2(x_2^*)]^2} > 0. \tag{29}$$

Partial differentiation of λ_1 with respect to J_2 shows that λ_1 monotonically increases with J_2 when $J_2 F_2(x^*) > 1 + J_1 F_1(u^*)$. Therefore, we can observe a bistable repression cascade if we increase the resource sequestering capability of node 2 ($J_2 F_2(x^*)$) and decrease that of node 1 ($J_1 F_1(u^*)$). Physically, these conditions increase the amount of resources released by node 2 upon repression from x_1, which effectively "activates" the production of x_1, promoting the hidden positive auto-regulation (Fig. 7A). Full mechanistic model simulation using ODEs and resource conservations in Section III confirms that this deterministic system is bistable in some parameter and input ranges (Fig. 7B). Conversely, from (29), we can remove bistability by adding a sufficiently strong negative auto-regulation to node 1 such that $\partial G_1 / \partial x_1 < \gamma_1$, which ensures monostability.

Resource-limitation-induced bistability can potentially explain the experimental results in [14]. The authors observed bimodal distribution of protein concentrations at the output of a repression circuit, which disappears when negative auto-regulation is added to the cascade. However, bimodal distribution can stem from a number of other sources in addition to deterministic bistability, such as transcriptional and translational bursts [15]. Further theoretical and experimental work is required to verify the source of bimodality in this experiment.

VI. DISCUSSION AND CONCLUSION

In this work, we have developed a general modeling framework to describe the dynamics of gene networks in a resource-limited environment. The model reveals a hidden layer of interactions among nodes in the network, which have been largely neglected so far but will become more relevant when resources are limited. Such hidden interac-

TABLE II. SIMULATION PARAMETERS ($i = 1, 2$)

	y_T	z_T	$p_{1,T}$	$p_{2,T}$	K_1'	K_2'	K_1	K_2	$\delta_i = \omega_i$	γ_i	θ_i	α_i	n	m	k_1	k_2	κ_1	κ_2
Unit	nM	μM	nM	nM	μM	μM	μM	μM	hr^{-1}	hr^{-1}	hr^{-1}	hr^{-1}	-	-	nM^n	nM^m	μM	μM
Fig.2	500	1	50	50	5×10^4	10^4	0.1	10	10	1	500	200	2	4	10	1000	1	100
Fig.5	100	1	-	-	200	100	1	1	10	1	200	200	2	4	100	100	-	10
Fig.7A	500	1	50	-	2	0.2	$\times$	$\times$	20	2	200	200	2	4	100	100	100	-
Fig.7B	50	0.5	50	200	2	0.1	$\times$	$\times$	20	5	100	350	1	4	10	1	10	1

tions can alter the steady state I/O response or stability of a network, as we have demonstrated in the examples of activation and repression cascades. Experimental validation of our results is currently underway in our lab.

A real cell system has a number of additional complications that are not included in our model. Firstly, recent evidence suggests that resources are not distributed evenly in cells [16]. How spatial distribution of resources changes our current results need to be investigated. Secondly, when exogenous circuits are overly activated, living cells tend to reduce the production of ribosomal proteins and produce heat shock proteins [16]. The redistribution of cellular resources under these conditions involves some regulation mechanisms that are still unknown and not accounted for in this resource conservation model. Moreover, although the key limiting factors appeared to be RNAP and ribosome [17], [18], resource sharing occurs at all levels of protein production. For instance, it is well known that RNAP compete for σ-factors [5]. Finally, when molecular counts are too low, instead of using ODE models, it is necessary to adopt stochastic modeling [2]. In future work, we will analyze to what extent these additional considerations need to be factored into the model.

Acknowledgement: We thank Eduardo D. Sontag, Abdullah Hamadeh, Hsin-Ho Huang and Andras Gyorgy for helpful discussions and suggestions.

APPENDIX

The dissociation constant of T7 RNAP binding with promoter is $K = 220$[nM] [19]. T7 RNAP has stronger binding with promoters than other RNAP species [20], therefore, $K \gg 220$ [nM]. Furthermore, since $y < y_T \approx 100$[nM] [3], we can assume $y \ll K$. Physically, this corresponds to the fact that promoters are rarely occupied by RNAP, which is common in experiments. For instance, Chrchward et al. find that DNA template is in excess of free RNAP in constitutively expressing *lac* genes [18]. The free amount of ribosome in *E. coli* is estimated to be $z < z_T \approx 1000$[nM] [3] at low growth rate of 1 doubling/hr, and a typical value of RBS dissociation constant is $\kappa \approx 5000$[nM] [21], which suggests $z \ll \kappa$. These assumptions are closer to reality when the network is larger in scale, and thus resources become more scarce.

REFERENCES

[1] S. Cardinale and A. P. Arkin, "Contextualizing context for synthetic biology- identifying causes of failure of synthetic biological systems," *Biotechnol. J.*, vol. 7, pp. 856–866, 2012.

[2] D. Del Vecchio and R. M. Murray, *Biomolecular Feedback Systems*. Princeton University Press, 2014.

[3] H. Bremer and P. P. Dennis, "Modulation of chemical composition and other parameters of the cell by growth rate," in *Escherichia coli and Salmonella: Cellular and Molecular Biology*, F. C. Neidhardt, Ed. ASM Press, 1996.

[4] T. H. Segall-Shapiro, A. J. Meyer, A. D. Ellington, E. D. Sontag, and C. A. Voigt, "A resource allocator for transcription based on a highly fragmented T7 RNA polymerase," *Mol. Syst. Biol.*, vol. 10, p. 742, 2014.

[5] D. De Vos, F. J. Bruggeman, H. V. Westerhoff, and B. M. Nakker, "How molecular competition influences fluxes in gene expression networks," *PLoS ONE*, vol. 6, no. 12, p. e28494, 2011.

[6] E. Yeung, J. Kim, and R. M. Murray, "Resource competition as a source of non-minimum phase behavior in transcription-translation systems," in *Proceedings of the 52nd IEEE Conference on Decision and Control*, 2013, pp. 4060–4067.

[7] A. Gyorgy and D. Del Vecchio, "Limitations and trade-offs in gene expression due to competition for shared cellular resources," in *Proceedings of the 53rd IEEE Conference on Decision and Control*, 2014.

[8] A. Hamadeh and D. Del Vecchio, "Mitigation of resource competition in synthetic genetic circuits through feedback regulation," in *Proceedings of the 53rd IEEE Conference on Decision and Control*, 2014.

[9] U. Alon, *An Introduction to Systems Biology: Design Principles of Biological Circuits*. Chapman & Hall/CRC Press, 2006.

[10] A. Gyorgy and D. Del Vecchio, "Modular composition of gene transcription networks," *PLoS Comput. Biol.*, vol. 10, no. 3, 2014.

[11] D. Kim, Y.-K. Kwon, and K.-H. Cho, "The biphasic behavior of incoherent feed-forward loops in biomolecular regulatory networks," *Bioessays*, vol. 30, no. 11-12, pp. 1204–1211, 2008.

[12] R. Thomas, "On the relation between the logical structure of systems and their ability to genegene multiple steady states or sustained oscillations," *Springer Series in Synergetics*, vol. 9, pp. 180–193, 1981.

[13] E. M. Ozbudak, M. Thattai, H. N. Lim, B. I. Shraiman, and A. van Oudenaarden, "Multistability in the lactose utilization network of Escherichia coli," *Nature*, vol. 427, pp. 737–740, February 2004.

[14] Y. Dublanche, K. Michalodimitrakis, N. Kümmerer, M. Foglierini, and L. Serrano, "Noise in transcription negative feedback loops: Simulation and experimental analysis," *Mol. Syst. Biol.*, vol. 2, p. 41, 2006.

[15] M. Kærn, T. C. Elston, W. J. Blake, and J. J. Collins, "Stochasticity in gene expression: from theories to phenotypes," *Nat. Rev. Genet.*, vol. 6, pp. 451–464, June 2005.

[16] D. J. Jin, C. Cagliero, and Y. N. Zhou, "Growth rate regulation in Escherichia coli," *FEMS Microbiol. Rev.*, vol. 36, pp. 269–287, 2012.

[17] J. Vind, M. A. Sørensen, M. D. Rasmussen, and S. Pedersen, "Synthesis of proteins in Escherichia coli is limited by the concentration of free ribosomes: Expression from reporter gene does not always reflect functional mRNA levels," *J. Mol. Biol.*, vol. 231, pp. 678–688, 1993.

[18] G. Churchward, H. Bremer, and R. Young, "Transcription in bacteria at different DNA concentrations," *J. Bacteriol.*, vol. 150, no. 2, pp. 572–581, 1982.

[19] V. L. Tunitskaya and S. N. Kochetkov, "Structural-functional analysis of bacteriophage T7 RNA polymerase," *Biochemistry (Moscow)*, vol. 67, no. 10, pp. 1124–1135, 2002.

[20] S. Tabor, "Expression using the T7 RNA polymerase/promoter system," *Current Protocols in Molecular Biology*, vol. 11:I:16.2, pp. 16.2.1–16.2.11, 2001.

[21] D. Kennell and H. Riezman, "Transcription and translation initiation frequencies of the Escherichia coli lac operon," *J. Mol. Biol.*, vol. 114, no. 1, pp. 1–21, 1977.